Available online at www.sciencedirect.com
ScienceDirect
Journal of Chromatography B, 858 (2007) 106–117
JOURNAL OF CHROMATOGRAPHY B
www.elsevier.com/locate/chromb

Normal phase and reverse phase HPLC-UV-MS analysis of process impurities for rapamycin analog ABT-578: Application to active pharmaceutical ingredient process development

Yong Chen [a,*], Gregory M. Brill [a], Nancy J. Benz [a], M. Robert Leanna [b], Madhup K. Dhaon [b], Michael Rasmussen [b], Casey Chun Zhou [c], James A. Bruzek [a], John R. Bellettini [b]

[a] *D-R45T, Process Analytical Chemistry, Global Pharmaceutical Research and Development, Abbott Laboratories, North Chicago, IL 60064-4000, USA*
[b] *D-R450, Process Chemistry, Global Pharmaceutical Research and Development, Abbott Laboratories, North Chicago, IL 60064-4000, USA*
[c] *D-R418, Structural Chemistry, Global Pharmaceutical Research and Development, Abbott Laboratories, North Chicago, IL 60064-4000, USA*

Received 5 February 2007; accepted 12 August 2007
Available online 21 August 2007

Abstract

ABT-578, an active pharmaceutical ingredient (API), is a semi-synthetic tetrazole derivative of the fermented polyene macrolide rapamycin. Reverse phase (RP)-HPLC-UV-MS and normal phase (NP)-HPLC-UV-MS methods employing an LC/MSD trap with electrospray ionization (ESI) have been developed to track and map all significant impurities from the synthetic process. Trace-level tracking of key impurities occurring at various process points was achieved using complimentary methodologies, including a stability indicating reverse phase HPLC method capable of separating at least 25 starting materials and process-related impurities from the API (YMC-Pack Phenyl column, UV-MS, 210 nm) and a targeted reverse phase HPLC method capable of separating very polar compounds from crude reaction mixtures (Phenomenex Synergi Polar RP column, UV, 265 nm). In addition, a normal phase HPLC method condition with post-column modifier infusion is described for the separation of epimeric impurities, and analysis of aqueous-sensitive reactive species (YMC-Pack SIL column, UV-MS, 278 nm). Process control strategies were established with these combinations of analytical technologies for impurities analyses to enable a rich understanding of the ABT-578 process.

Keywords: Drug-eluting stent; Zotarolimus; ABT-578; Rapamycin; Sirolimus; RP-HPLC-UV-MS; NP-HPLC-UV-MS; Process impurities; API process analytical development; Impurities tracking and mapping; HPLC impurity profile

1. Introduction

ABT-578 (zotarolimus), a tetrazole containing semi-synthetic rapamycin (sirolimus) analog, is the API for *ZoMaxx*™ and *Endeavor*™ drug-eluting stent devices. Elution of ABT-578 from these devices into surrounding vascular structures blocks cell proliferation, preventing scar tissue formation and minimizing restenosis in angioplasty patients [1,2]. Determination of the genesis, identification and fate analysis of impurities is central to developing a deep understanding of the commercial manufacturing process. Tracking impurities in the ABT-578 manufacturing process is very challenging due in past to the API's complex polyene macrolide structure including 15 stereogenic centers. The semi-synthetic process also introduces a number of process-related impurities resulting from side-product formation inherent in the highly reactive triflate intermediate required for the transformation of rapamycin to ABT-578. For example, multiple epimeric impurities can result from sigmatropic rearrangements at C-40 upon formation of the reactive rapamycin triflate. Additionally, the triene moiety can invite auto-oxidation during processing, and other degradative pathways of the ABT-578 core during bulk purification (e.g., macrocyclic ring opening). It is well known, for example, that polyene macrolides undergo radical-initiated oxidative degradation cascades when in amorphous form and unprotected by an anti-oxidant [3]. The ABT-578 process generally consists of reaction stages and large-scale chromatographic purification stages. ABT-578 is protected in production and storage through

* Corresponding author. Tel.: +1 847 935 6404.
E-mail address: yong.chen@abbott.com (Y. Chen).

1570-0232/$ – see front matter © 2007 Elsevier B.V. All rights reserved.
doi:10.1016/j.jchromb.2007.08.012

the addition of small amounts of butylated hydroxy toluene (BHT) anti-oxidant. While the utilization of this stabilizer greatly reduces the emergence of oxidative by-products during processing and storage, numerous low-level impurities are still observed from other pathways originating throughout the process, some of which can carry into final API. The process-related impurity profiles and API impurity profiles can be complex with impurities that are difficult to distinguish from each other.

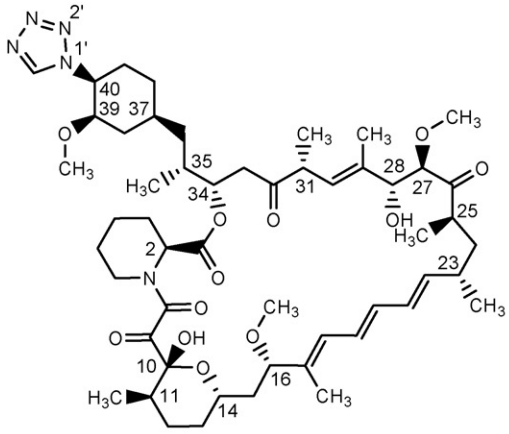

ABT-578: 40-Epi-(N1-tetrazolyl)-rapamycin
Numbering C-atoms per IUPAC

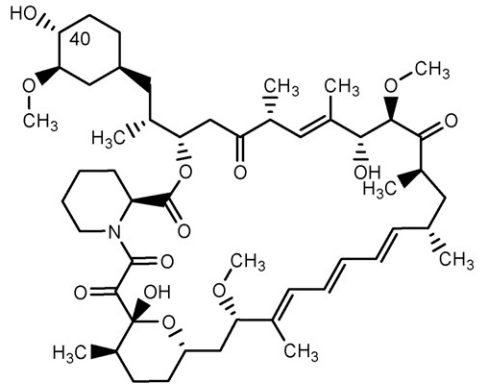

Rapamycin

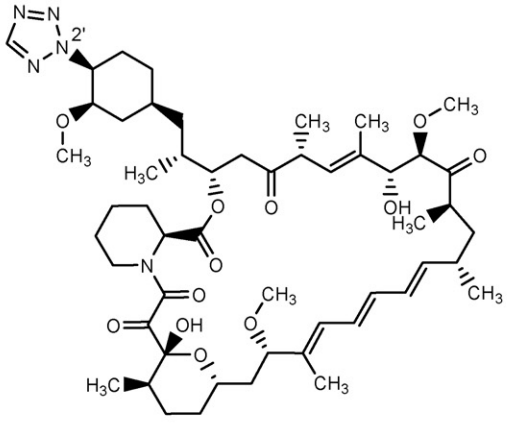

N2 Isomer

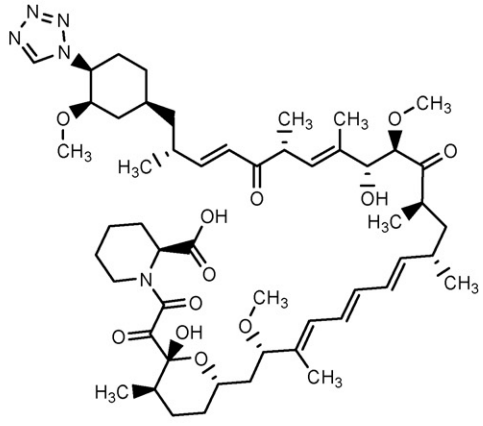

Open Ring Acid

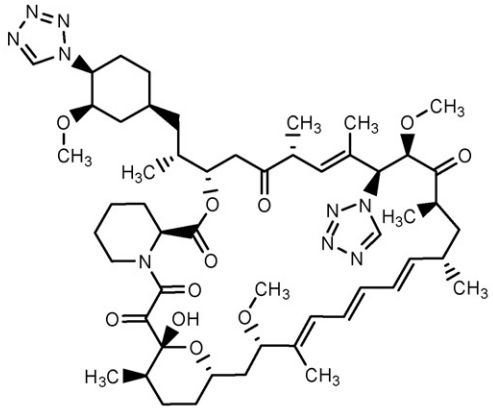

Ditetrazole of ABT-578

Fig. 1. Structure of ABT-578 (15 chiral centers, subject to multiple epimerizations from chemical, thermal or photo reactiveness, structures of process epimer impurities not shown). Epimers: diastereoisomers that have the opposite configuration at only one chiral center of multiple chiral centers.

Different aspects of impurity studies, ranging from method development to impurity identification techniques, have been extensively reported and reviewed in the literature [4–8]. A main goal in early-stage pharmaceutical development is to prudently and quickly establish a scaled-up synthetic process for making acceptable API. In this regard, analytical impurities methods used for both in-process and API release testing must rapidly evolve to account for the detection and quantification of all key impurities—matching the speed of a developing and changing process. Mass spectrometry detection capability coupled with HPLC is an important tool and there are numerous examples that demonstrate its application to issues associated with process development for new pharmaceutical products [9–11]. It is frequently a proceeding, and many times sufficient step before undertaking painstaking isolation and enrichment of impurities for NMR identification. The most difficult thing during chromatographic method development is accurately tracking peaks from various different columns and conditions [12]. The authors have found that the insight gained from using HPLC-UV-MS as a general research strategy during process development quickly yields substantial benefits in terms of more efficient and complete enabling of process understanding. With ABT-578, for example, there are generally no particular impurities that dominate the final API impurity profile, but multiple process impurities and isomers/epimers are generated (see more discussion in Section 3.5). The impurity profile from the process to final API is extensive and consists of impurities that are structurally very close to ABT-578, such as those examples shown in Fig. 1. ABT-578 is named as 40-Epi-(N1-tetrazolyl)-rapamycin and the C-atoms are numbered per IUPAC guidelines [13]. In recent years, the hyphenation of mass spectrometer to HPLC analyses has become increasingly common for process-related impurities tracking. Successful peak tracking based on molecular weights enables the correlation of results from multiple orthogonal methods, building comprehensive impurity profiles for pharmaceutical samples as long as the impurities do not have iso-mass ions with respect to the analyte [14]. However, even iso-mass peaks provide differential information related to other process impurities. To our knowledge, there are no literature reports on analytical control of a semi-synthetic process regarding macrolide compounds.

In order to develop a comprehensive understanding of the manufacturing process, and implement meaningful analytical HPLC-UV controls for production (UV detection normally used in production laboratories [15]), a research method strategy was focused on tracking numerous individual impurities through the control points to API with MS detection. In this article, we present a comprehensive process impurity tracking approach. This was achieved by developing a combination of complimentary HPLC-UV-MS methods to effectively monitor the creation and fate of all individual impurities (for process development purposes). Strategies included the use of combined analytical technology to achieve the best possible separation of all process impurities with the fewest control methods (three), track most process impurities, including reactive intermediates and isomers/epimers, through the process by NP-HPLC-UV-MS, develop a targeted RP-HPLC-UV method for transient or polar process impurities, and establish a stability indicating RP-HPLC-UV-MS impurities method for API. The use of MS detection greatly facilitated tracking impurities, using both UV and molecular ion, correlating impurities across different methods and process points. A flowchart of synthesis and purification steps for ABT-578 is shown in Fig. 2a and an interrelationship flowchart of the process with the three methods is shown in Fig. 2b. ABT-578 synthetic methods have been reported previously [16–19]. The resultant studies led to better analytical controls coupled with optimized reaction and purification procedures, providing for more efficient production of ABT-578.

2. Experimental

Inspection of the structure of ABT-578 reveals several intrinsic challenges with respect to monitoring the synthetic process. These challenges include monitoring the integrity of multiple stereogenic centers, and the realized possibility of regiochemical impurities on both the tetrazole and the polyene macrocyclic skeleton (Fig. 1). Furthermore, each ABT-578-related pyran compound can have a complimentary equilibrium isomer of oxepane form in low-level thermodynamic ratio under RP chromatographic conditions (Fig. 3). The equilibrium oxepane

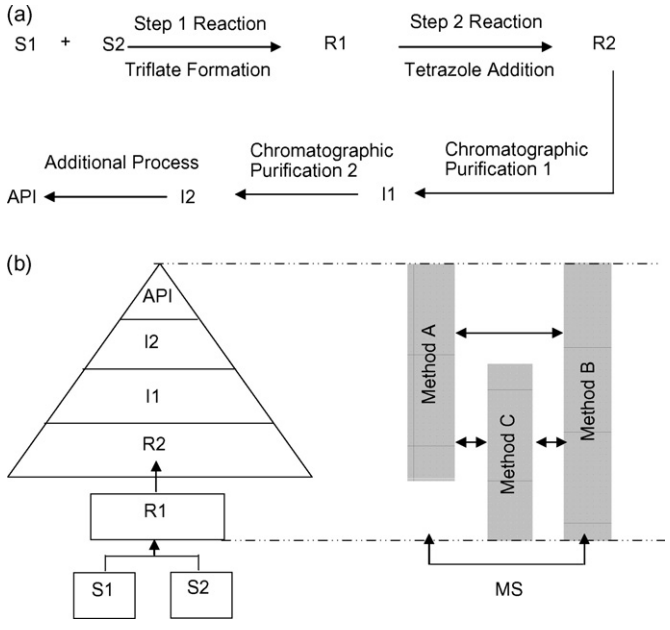

Fig. 2. (a) ABT-578 synthesis and purification process flowchart: S1 and S2, starting materials; R1, triflate formation, reaction mixture; R2, tetrazole addition, reaction mixture; I1, intermediate, chromatography on silica gel, impurities removed or generated from R2; I2, intermediate, chromatography on silica gel, impurities removed or generated from I1; and ABT-578, final API. (b) Interrelationship flowchart of process impurity controls with use of three HPLC methods: Method A for general impurities tracking from R2 to API; Method B for epimer impurities tracking from R1 to API and reactive intermediate tracking in R1 and R2; Method C for polar impurities tracking from R1 to I1 (up to API if needed); MS detection: facilitated process impurities tracking and mapping (upwards of 60–70 impurities); box size: relative impurities levels at points of the process.

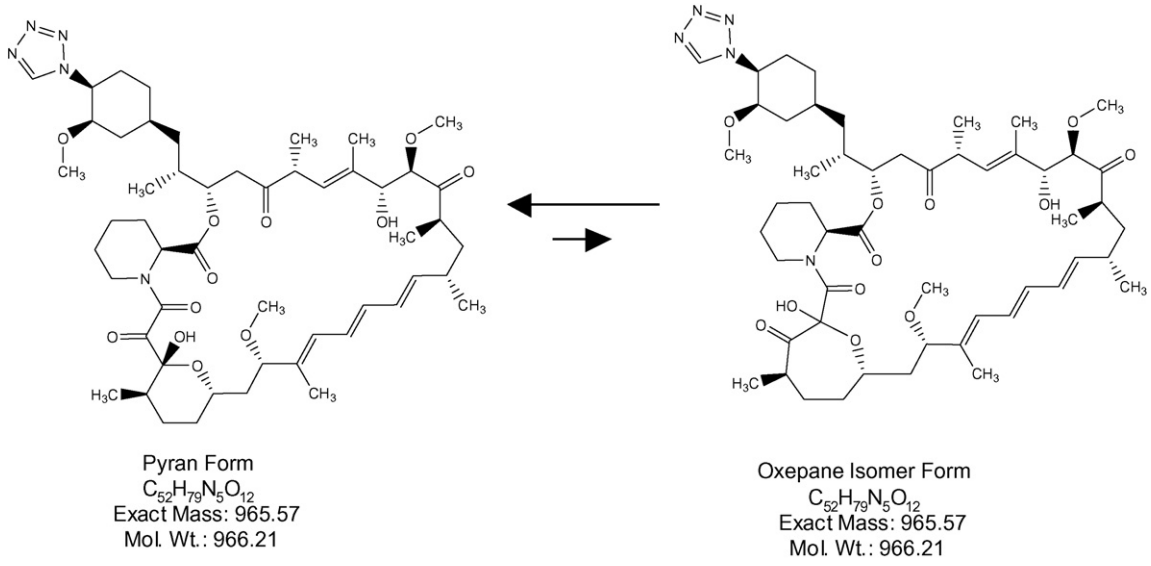

Fig. 3. Pyran and oxepane structures of ABT-578 (equilibrium isomers in solution).

isomer of ABT-578 is also reported and discussed in the literature [20]. The rapamycin/ABT-578 triene moiety absorbs at UV lambda max of 276–278 nm, but it was determined that some important degradation impurities were not detected at this wavelength. Efforts to address these challenges, detailed below, included: (a) development of a stability indicating RP-HPLC-UV-MS method for ABT-578-related impurity profile studies; (b) development of a NP-HPLC-UV-MS method for stereo-isomer control and targeted reaction monitoring of aqueous-sensitive process impurities; and (c) development of a targeted RP-HPLC-UV impurity method for studies of polar impurities in complicated reaction matrixes. Method conditions and example studies involving tracking of key process impurities are provided. ABT-578 and the impurity structures shown in this paper had identifications confirmed by NMR and proprietary structures are omitted.

2.1. Reagents and materials

ACS grade ammonium acetate was purchased from J.T. Baker (Philipsburg, NJ, USA). HPLC grade methanol (MeOH), acetonitrile (MeCN), tetrahydrofuran (THF), and *n*-heptane were purchased from EMD Chemicals (Gibbstown, NJ, USA). Water was obtained from a Milli-Q ultra pure water purification system from Millipore (Bedford, MA, USA). ABT-578, rapamycin, and BHT were obtained from Abbott Laboratories Reference Standards.

2.2. Instrumentation

The HPLC system was an Agilent 1100 series with autosampler and column heater (Palo Alto, CA, USA). The MS system was an Agilent LC/MSD Trap SL (Palo Alto, CA, USA). An accurate post-column splitter from LC Packing (San Francisco, CA, USA) was used between the outlet of the UV detector and the inlet of the MS detector. Agilent MSD Trap control software version 5.0 (Palo Alto, CA) was used for MS data acquisition and data processing. The infusion pump for NP-HPLC-MS was a KDS100 from KD Scientific (Holliston, MA, USA). A six-column selector from Phenomenex (Torrance, CA, USA) was also used as part of method development for column screening.

2.3. Chromatographic conditions for main HPLC-UV-MS methods

2.3.1. Method A: RP-HPLC-UV-MS, 210 nm, for ABT-578-related substances and general impurities

A YMC-Pack phenyl column (4.6 mm × 25 cm, 5 μm) was used with gradient elution from mobile phase A (MPA) consisting of buffer (10 mM ammonium acetate, pH 4.0)–water–MeCN–MeOH (30:16:44:10) to mobile phase B (MPB) consisting of buffer–MeCN–MeOH (30:63.5:6.5) at a flow rate of 1.0 mL/min. The column temperature was maintained at 45 °C and the autosampler temperature was set at 4 °C. The ABT-578 sample solution was injected at a concentration of approximately 2.2 mg/mL with an injection volume of 20 μL. The gradient conditions for the method are listed below.

Time (min)	MPA (%)	MPB (%)
0.0	100	0
55.0	0	100
56.0	100	0
68.0	100	0

MS detection using ESI, operated in both positive and negative mode, was used to help identify molecular ions and track unknown impurities. Post-column stream splitting was used with a 1–10 split to increase sensitivity by reducing background interference from excessive mobile phase (1 volume to MS detection and 10 volumes to waste). MS instrument tuning was performed with an ABT-578 standard

from post-column infusion to ensure the highest sensitivity. The trap drive was set at 69 V, drying temperature at 325 °C, nebulizer gas at 10 psi, drying gas flow at 5.00 L/min, scan speed at *m/z* 13,000 s^{-1}, and scan range (*m/z*) at 100–2200.

2.3.2. Method B: NP-HPLC-UV-MS, 278 nm, for screening process samples and API

A YMC-Pack SIL column (4.6 mm × 25 cm, 5 μm) was used with gradient elution from MPA consisting of *n*-heptane to MPB consisting of THF (BHT free) at a flow rate of 1.0 mL/min. The column temperature was maintained at 50 °C and the sample tray temperature was set at 4 °C. ABT-578 sample solution was injected at a concentration of approximately 1 mg/mL with an injection volume of 5 μL. The gradient conditions for the method are listed below.

Time (min)	MPA (%)	MPB (%)
0.0	74	26
40.0	50	50
55.0	10	90
56.0	74	26
70.0	74	26

MS detection using ESI, operated in both positive and negative mode, was used to identify additional unknown impurities. To offset poor ionization with THF/*n*-heptane, a 1–20 post-column stream splitting of the mobile phase out of the UV detector was used. In addition to the splitting, a post-infusion pump was also introduced to add a modifier at the rate of 500 μL/h consisting of buffer (10 mM ammonium acetate, pH 4.0)–MeCN–MeOH (12.5:12.5:75) to the THF/*n*-heptane eluent. Instrument tuning was performed with post-column modifier infusion to ensure the highest sensitivity. The trap drive was set at 69 V, drying temperature at 325 °C, nebulizer gas at 10 psi, drying gas at 5.00 L/min, scan speed at *m/z* 13,000 s^{-1}, and scan range (*m/z*) at 100–2200.

2.3.3. Method C: RP-HPLC-UV, 265 nm, for polar impurities of process samples and API

A Phenomenex Synergi Polar RP column (4.6 mm × 25 cm, 5 μm) was used with gradient elution from MPA consisting of 0.25 mM ammonium acetate buffer (pH 4.0) to MPB consisting of 100% MeCN at a flow rate of 1.0 mL/min. The column temperature was maintained at 45 °C and the autosampler temperature was set at 4 °C with an injection volume at 5 μL. The main purpose of Method C is to track and quantify polar impurities in complex reaction matrixes and purification processes (Fig. 2a, R1, R2, and I1). Therefore, the linearity of polar impurities from 0.6 to 22 μg/mL was needed, and was established, with a minimum regression correlation coefficient of 0.9999 for each. With this wide linearity range, quantification of various levels of polar impurities at different process points was achieved. The gradient conditions for the method are listed below.

Time (min)	MPA (%)	MPB (%)
0.0	90	10
25.0	75	25
25.5	5	95
44.0	5	95
44.5	90	10
55.0	90	10

MS detection was not necessary for Method C because of acceptable polar impurity separation and tracking using only UV detection.

3. Results and discussion

3.1. Method development for tracking and mapping ABT-578 in-process and final API impurities

RP-HPLC is generally more applicable for analytical pharmaceutical analyses than other types of HPLC. The columns are efficient, reproducible, stable and UV-MS detection is easier with the solvents used. Structural isomers can be separated in many cases by RP-HPLC. Method A (RP-HPLC-UV-MS, 210 nm) was developed and used as the primary procedure for total impurity analyses of ABT-578. However, historically, the separation of closely-related isomeric or epimeric mixtures often require NP-HPLC than RP-HPLC due to the differences in aligning their polar function groups with adsorption sites (somewhat like a lock and key fit) [21]. With the range and complex nature of ABT-578 impurities (crude reaction mixture through the downstream purification process; refer to Fig. 2a and b), development of a single suitable method to comprehensively profile all impurities was not realistic. Since tracking and mapping impurities were essential for comprehensive understanding of each impurity's fate, including reactive species, Method B (NP-HPLC-UV-MS, 278 nm) was selected as an additional research methodology. Finally, Method C (RP-HPLC-UV, 265 nm) was used for analysis of highly polar impurities from crude reaction mixtures. All three methods are amenable to and capable of MS detection.

3.2. Method A development

Initial ABT-578 HPLC methodology was based on a Zorbax Eclipse, XDB-C8 column (4.6 mm × 25 cm, 5 μm) with detection at 278 nm and gradient elution from MPA consisting of buffer (10 mM ammonium acetate, pH 4.0) to MPB consisting of MeCN at a flow rate of 1.0 mL/min. The column temperature was set at 45 °C, autosampler temperature at 4 °C. The ABT-578 sample solution was at a concentration of approximately 0.5 mg/mL with an injection volume of 50 μL. The gradient conditions for the method are shown below.

Time (min)	MPA (%)	MPB (%)
0.0	50	50
65.0	30	70
66.0	50	50
75.0	50	50

This method was adequate enough as a stability indicating method to separate most general impurities for API analysis, but could not meet API process development demands because of two main issues: (1) BHT invariably co-eluted with impurities eluting after ABT-578, and (2) some degradation impurities generated in the process could not be detected at 278 nm. Subsequently, a YMC phenyl column (4.6 mm × 25 cm, 5 μm) (enhancing phenyl selectivity compared with XDB-C8 column) was selected with addition of MeOH (enhancing *pi–pi* interactions) to the mobile phase. The gradient was also adjusted. As a result, elution order for BHT relative to the main component was reversed and BHT was separated from all other impurities while preserving the elution profile of other impurities, with minimized impact to the general impurity profile. The gradient conditions are shown below.

Time (min)	MPA (%)	MPB (%)
0.0	99	1
55.0	65	35
56.0	99	1
68.0	99	1

However, because of unbalanced ammonium acetate buffer concentration (preferred because of enhanced MS signals used to track trace level impurities) in MPA and MPB during the gradient, use of a lower UV detection wavelength was problematic. Thus, the final changes were a balanced buffer concentration between MPA and MPB, and a change of the detection wavelength to 210 nm, creating Method A. Fig. 4a–c shows chromatogram comparisons for the method's evolution using the same lot of ABT-578 API sample, showing similar impurity profiles. Relative retention time (RRT) to ABT-578 1.24–1.33 impurities are indicated in the chromatogram for understanding of tracking and mapping discussed in Section 3.5.

3.3. Method B development

Manipulating selectivity for ABT-578 impurities that differ by molecular weight or gross macrocyclic structure (e.g., by adding/losing a methyl, additional tetrazole, or ring opened) is reasonably achievable when using reverse phase conditions, but not so with normal phase conditions. However, normal phase conditions afford selective windows of separation for certain closely related ABT-578 isomers/epimers by exploiting differ-

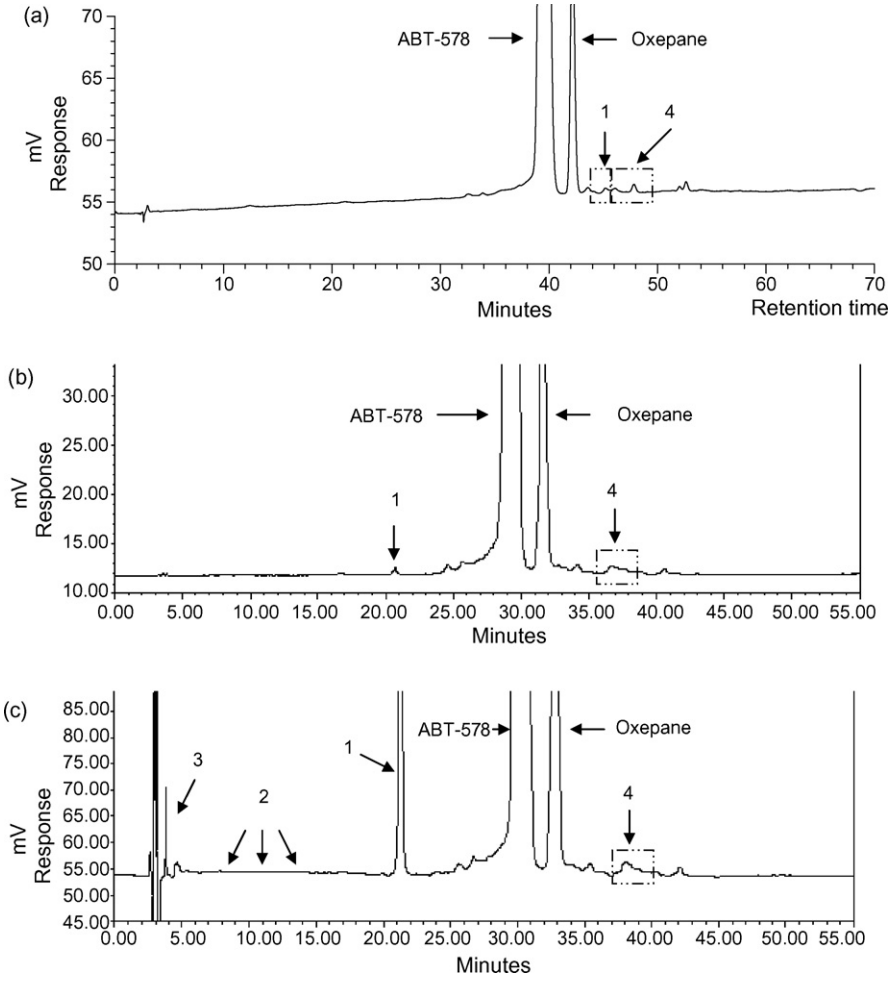

Fig. 4. (a) ABT-578 API and related substances with C8 column at UV 278 nm: partial co-elution of BHT (1) with ABT-578-related impurities and RRT 1.24–1.33 impurities (4). (b) ABT-578 API and related substances with phenyl column at UV 278 nm: separation of BHT (1) from ABT-578-related impurities and RRT 1.24–1.33 impurities (4). (c) Method A: ABT-578 API and related substances with phenyl column at UV 210 nm: separation of API potential polar impurities (3), potential process degradation impurities (2), and BHT (1) (much higher UV response compared with 278 nm) from ABT-578-related impurities, and RRT 1.24–1.33 impurities (4). *Note*: RRT 1.24–1.33 impurities were discussed in Section 3.5.

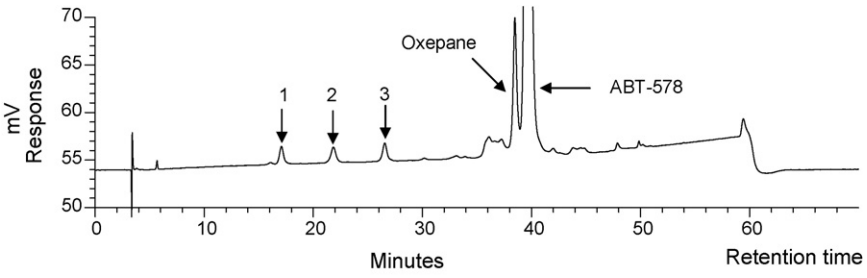

Fig. 5. Method B: separation of a N2 isomer (1), an isomer of rapamycin (2), and rapamycin (3) (1% spiking of each impurity) from ABT-578 in normal phase analysis.

ences in alignment of polar functional groups with adsorption sites on the column packing. In fact, Method A separates most general API impurities, but falls short for in-process samples containing close isomers of rapamycin and close API-related isomers/epimers. Method A also has the disadvantage of aqueous conditions not amenable to analysis of aqueous-reactive process intermediates. Although most of these impurities are rejected during the process, tracking them in order to aid process optimization and control was critical. Method B was developed and optimized for isomer/epimers separations as well as the capability of detecting aqueous-reactive intermediates. The following are examples of Method B applied to in-process and API samples.

Example of API samples: with Method B, isomers of rapamycin and ABT-578 are successfully separated from ABT-578 with limit of quantitation (LOQ) of 0.04%. Fig. 5 illustrates the separation of an ABT-578 N2 isomer, an isomer of rapamycin, and rapamycin itself from ABT-578 API.

Example of tracking three major ABT-578 in-process epimer impurities: three major ABT-578 epimers are formed in the initial reaction and are rejected in further process purifications (refer to Fig. 2a and b, R1, R2, and I1). Under RP conditions, these epimers co-elute with ABT-578 or other impurities. With Method B, these impurities are successfully separated from ABT-578 for all in-process samples, enabling process monitoring and control. Fig. 6 illustrates the separation of these epimer impurities from ABT-578 in a crude reaction mixture (refer to Fig. 2a, R2). In addition, reactive intermediates generated in the crude reactions (refer to Fig. 2a, R1 and R2) that would decompose under aqueous RP conditions (one structural example in Fig. 7) are also separated from ABT-578 and other

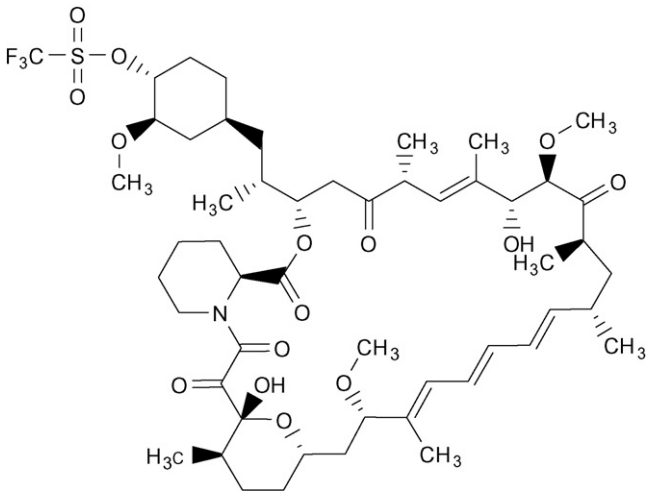

Fig. 7. Example structure of a reactive intermediate (triflate of rapamycin).

impurities. Monitoring levels of the reactive intermediates is important because the crude reaction mixture is placed directly into process chromatography purification. Method B can monitor levels of aqueous-reactive intermediates since the mobile phase is composed of aprotic solvents THF and *n*-heptane. Fig. 6 also illustrates the separation and detection of reactive intermediates for ABT-578 in a crude reaction mixture (refer to Fig. 2a, R2).

3.4. Method C development

Method B is an excellent compliment to Method A for tracking a range of process impurities as discussed above. However,

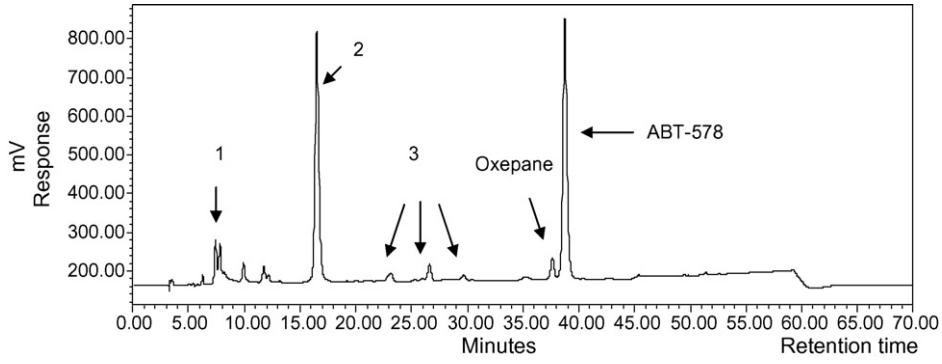

Fig. 6. Method B: separation of reactive intermediates (1), N2 isomer (2), and epimers of ABT-578 (3) from ABT-578 from a crude reaction example.

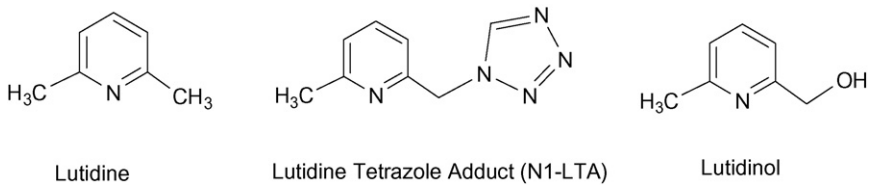

Fig. 8. Example structures of polar process impurities.

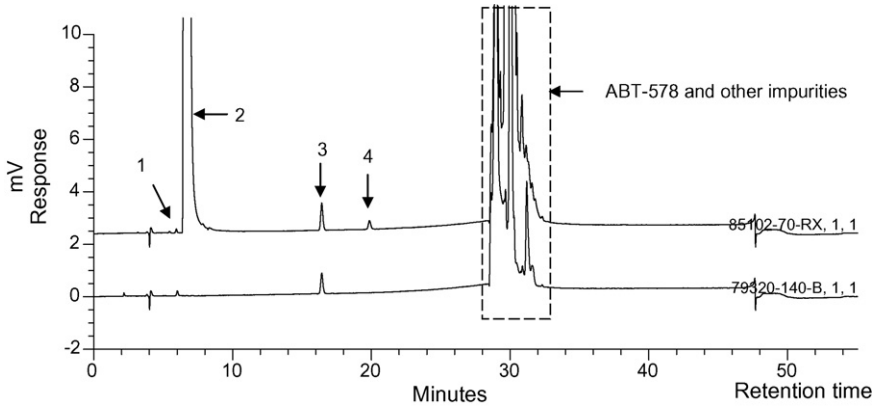

Fig. 9. Method C: comparison of polar impurities from a crude reaction mixture sample (top) to a further purification sample (bottom). *Notes*: Polar impurities lutidinol (1), luditine (2), N1-LTA (3), and N2-LTA (4) were separated from ABT-578 and related impurities, and polar impurities are removed in purification process. Quantitations were achieved on all polar impurities in matrixes.

for the very polar impurities generated early in the process, neither Method A nor B capture this final part of the full range in a crude reaction mixture. Fig. 8 shows some example structures of polar impurities in a crude reaction mixture. Although most of the critical polar impurities are rejected in the process (refer to Fig. 2a and b, R1 to API process), the collective levels of these impurities when present in the process can alter subsequent processing enough to impact the quality and yield of API. Therefore, Method C was developed as a targeted method optimized to cover these very polar impurities from reaction mixture stage to final API. This was achieved by employing a special polar RP column (Phenomenex Synergi Polar RP) to retain polar compounds under typical RP conditions. This ether-linked phenyl phase column specifically maximized the retention and selectivity for polar and aromatic compounds. Fig. 9 illustrates a chromatographic example of impurity rejection process from a crude reaction sample to a further purification process sample.

3.5. MS detection examples

HPLC with a single UV wavelength for detection is by far the most widely used technique to routinely track and quantify known impurities in industrial production laboratories. However, R&D laboratories use both DAD-UV and MS as complimentary approaches during method development and to build correlated knowledge to investigate known and unknown impurities.

MS detection is coupled with the previously described Methods A and B to track and map impurities, study co-elution of impurities and distinguish impurity peaks where UV detection alone would fall short. The purpose of this article is to illustrate the use of combined analytical technologies with MS detection as applied to efficient process development. A significant number of process impurities were isomers, epimers, and/or closely related analogs of ABT-578. With molecules of this size, and many closely eluting unknown impurities in process control methods, separation and identification by molecular ions is a priority in order to develop detailed understanding of what is happening from crude reaction mixtures to isolated API. Both negative and positive MS modes with ammoniate acetate addition were used (+18 for ammonium adduct in positive and +59 for acetate adduct in negative mode) in combination with UV, dramatically increasing the pace of tracking known and unknown impurities through the process. The detailed additional data it provided has led to better understanding and control of the ABT-578 process chemistry. The following examples illustrate the advantage it provided.

RRT 1.24–1.33 (refer to Fig. 4c) region impurities are observed in crude reaction mixture samples, further process purification samples, and API at significant levels using Method A. Without MS detection (production laboratories generally monitor by UV with no MS detection), an incorrect mapping conclusion can be made due to co-elution of differing impu-

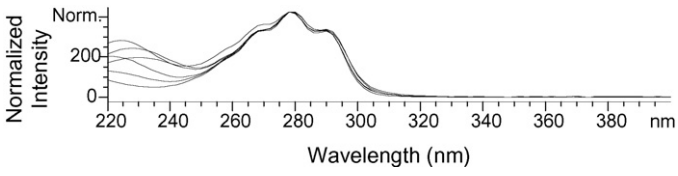

Fig. 10. UV diode-array of RRT 1.24–1.33 process impurities (Fig. 2a, I1) overlaid with that of ABT-578, similar triene UV spectrum.

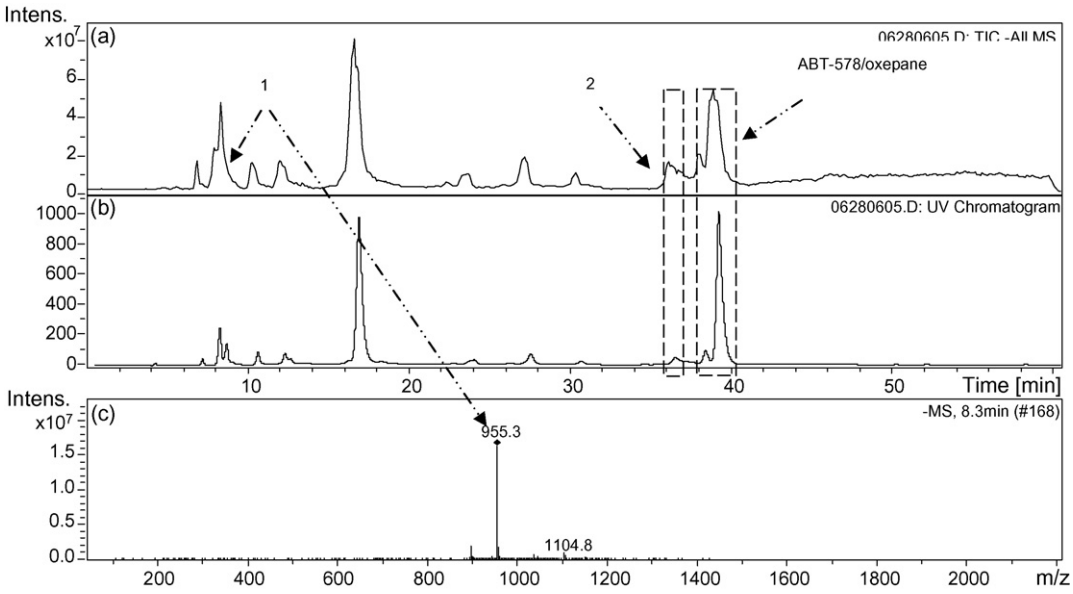

Fig. 11. Method A RRT 1.24–1.33 process impurities from a crude reaction mixture sample (Fig. 2a, R2) with Method B chromatography, (a) total ion chromatogram (TIC) with the separation of peak of interests (1) and (2) that co-eluted in Method A (Fig. 3c); (b) UV trace at 278 nm; (c) MS identification of MW 896 impurity (1) (*m/z* 955.5, +59 acetate adduct) and MW 966 impurity (2) (*m/z* not shown here).

rities from various process points (different sample matrixes) falling in this same chromatographic region. In this region, Fig. 10 shows the same UV diode-array response of a triene chromophore from a further purification sample that indicates all are related impurities to rapamycin or ABT-578. The same spectra in the region are also obtained from a crude reaction. When selectivity of closely eluting impurities is limited with UV alone, MS detection is then crucial for distinguishing dif-

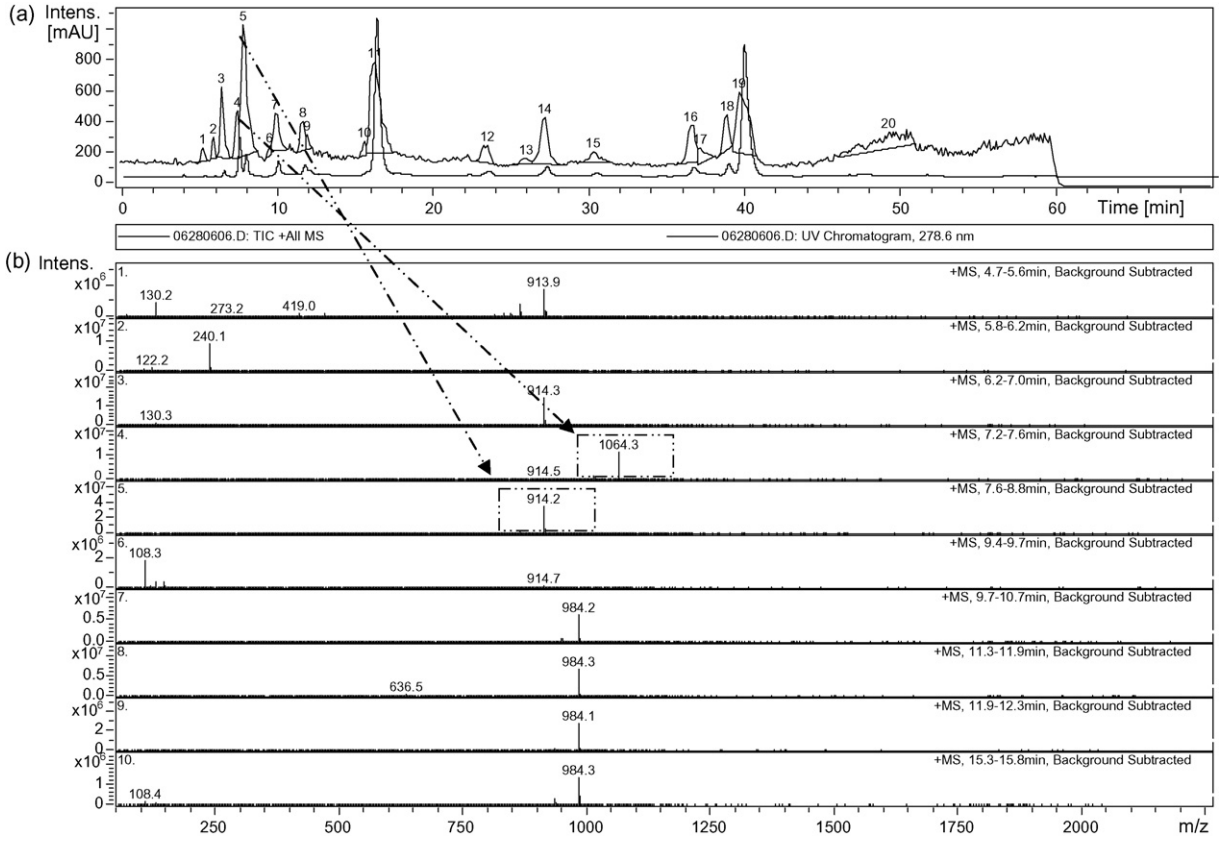

Fig. 12. Example of distinguishing reactive intermediate (arrows) among other impurities by Method B from a crude reaction mixture sample (Fig. 2a, R2), (a) total ion chromatogram in positive mode (top) with UV trace (bottom), (b) MS spectra tracked impurities. *Notes*: MW 1046 reactive intermediate (4, *m/z* 1064.3, +18 as ammonium adduct) was distinguished from MW 896 impurity (5, *m/z* 914.2, +18 as ammonium adduct). Other impurities (1–20) were also tracked and mapped.

fering impurities. Two co-eluting impurities illustrate the point. Samples pulled from throughout the process show the 'same peak' by UV and location in the RRT 1.24–1.33 region. However, process mapping with MS detection demonstrates that this peak contains different impurities that originate at different process points: a MW 896 impurity peak is detected in crude reaction samples, whereas a MW 966 isomer impurity peak is detected in the same RRT location in the API. In order to separate and further study impurities in the Method A 1.24–1.33 RRT window, Method B with MS detection was used. The separation of the MW 966 isomer impurity from MW 896 (*m/z* 955.3 in negative mode, +59 as acetate adduct) is shown in Fig. 11. The resultant combination of information from using these orthogonal methods for in-process sample tracking led to a clear picture of which related impurities are present at various process points. The tracking of RRT 1.23–1.33 impurities from crude reaction mixture to final API is shown in Table 1. With the separation of these impurities in Method B, tracking the levels of each impurity can be achieved from crude reaction to API. In addition, Method B was used to distinguish other targeted reactive intermediates (Fig. 7) that are not detectable with Method A. A MW 1046 (*m/z* 1064.3 in positive mode, +18 as ammonium adduct) reactive intermediate distinguished from a closely eluted impurity, a MW 896 (*m/z* 914.2 in positive mode, +18 as ammonium adduct) impurity, is also shown in Fig. 12.

Table 1
Method A RRT 1.24–1.33 process impurities mapping example with MS detected co-elution of impurities in different process points (different sample matrixes)

Impurities MS detected	Crude reaction	Further purification	API
896 impurity	Yes (major)	ND	ND
966 (isomer A)	Yes	ND	ND
966 (isomer B)	Yes	ND	ND
966 (isomer C)	Yes	Yes (major)	Yes
934 impurity	Yes	Yes	Yes
948 impurity	ND	Yes	Yes
1018 impurity	ND	Yes	Yes (major)

ND: not detected. *Notes*: 896 impurity was the major impurity in crude reaction (Fig. 2a, R2); isomer C was the major impurity in further purification process (Fig. 2a, I1); 1018 impurity was the major impurity in API.

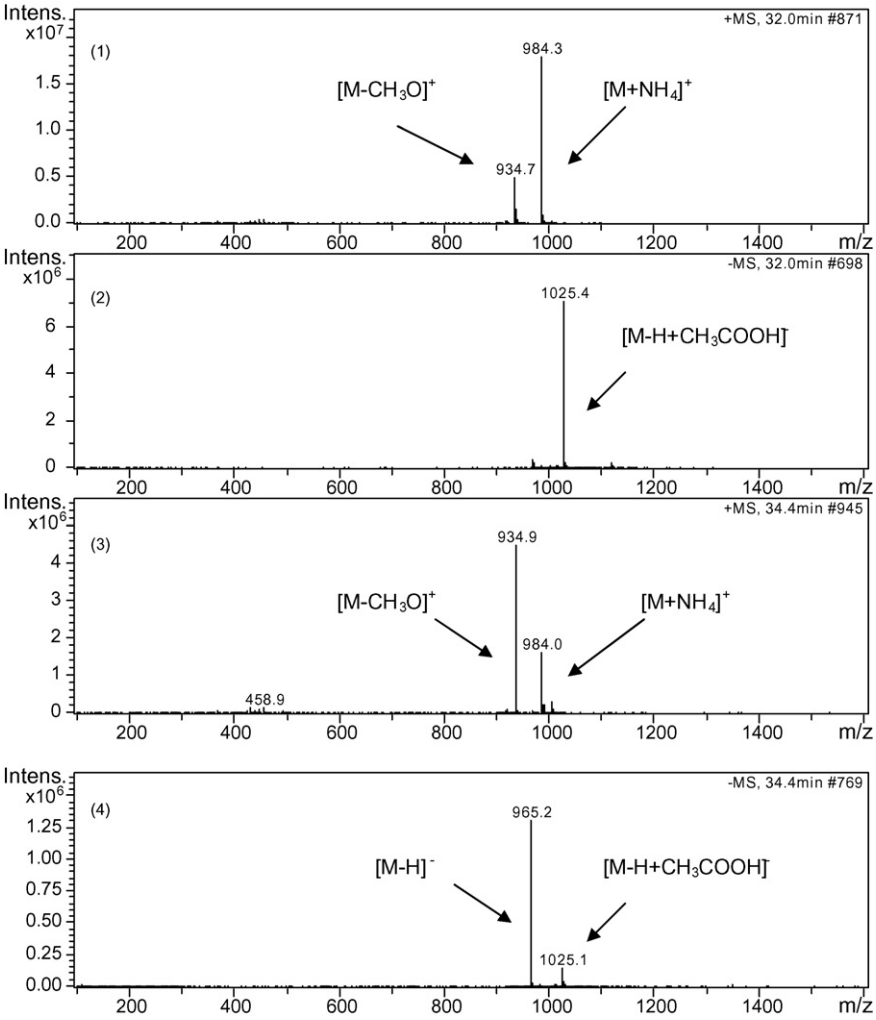

Fig. 13. MS spectra of ABT-578 with unique patterns and intensities of pyran and oxepane forms of ABT-578 (epimers show same patterns as ABT-578 on pyran and oxepane forms, as well as N2 isomers and their epimers), (1): ABT-578 pyran in positive mode, (2) ABT-578 pyran in negative mode, (3) ABT-578 oxepane in positive mode, and (4) ABT-578 oxepane in negative mode. LC and MS conditions (Method A) are described in Section 2.3.

Table 2
Mapping ABT-578 process impurities from early process to final API

Impurity	RRT (METH. A)	RRT (METH. B)	Detection (METH. C)	Formation	Rejection	API (METH. A)
Reactive intermediate A	N/A	0.186	N/A	Step 1	Step 2 Purification 1	ND
Reactive intermediate B	N/A	0.195	N/A	Step 1	Step 2 Purification 1	ND
Reactive intermediate C	N/A	0.204	N/A	Step 1	Step 2 Purification 1	ND
896 impurity A	1.24	0.166	N/A	Step 1	Purification 1	ND
896 impurity B	1.24	0.215	N/A	Step 1	Purification 1	ND
Polar impurity A	0.13	N/A	Y	Step 2 Purification 1	Purification 2	ND–LT 0.1
Polar impurity B	0.13	N/A	Y	Starting materials	Purification 2 Additional process	ND
Polar impurity C	0.14	N/A	Y	Step 2 Purification 1	Purification 1	ND–0.3
Polar impurity D	0.13	N/A	Y	Starting materials	Purification 1	ND
Degradation impurity A	0.27	N/A	N/A	Purification 1 Purification 2	Purification 1	ND–0.15
Degradation and process impurity A	0.58	N/A	N/A	Step 2	Purification 1	ND–LT 0.1
Degradation and process impurity B	0.66	N/A	N/A	Step 2	Purification 1	ND
Rapamycin	0.82	0.67	N/A	Starting materials	Purification 1	ND–0.1
Isomer of rapamycin	0.96	0.55	N/A	Step 2	Step 2	ND–0.3
Process impurity A	0.84	1.09	N/A	Starting materials	Purification 1	ND–0.3
Epimer impurity A	1.00	0.75	N/A	Step 2	Purification 1 Purification 2	ND–0.1
Epimer impurity B	1.08	0.68	N/A	Step 2	Purification 1 Purification 2	ND
Process impurity B	1.17	0.92 and 0.94	N/A	Step 2	Purification 2	LT 0.1–0.45
Process impurity C	1.28	0.92 and 0.94	N/A	Step 2	Purification 2	0.27–1.18

RRT: relative retention time to ABT-578 in each method; METH.: Method; N/A: not applicable; ND: same as in Table 1; LT: less than. *Note*: Refer to Fig. 2a and b for impurity formation and rejection during the synthesis and purification process.

Control of isomers/epimers is impossible without the combination approaches of Methods A and B coupled with MS detection. In the ABT-578 structure, there are at least four reactive sites (10, 28, 39, 40, Fig. 1). These sites are subject to possible formation of N2 isomers/epimers, in addition to ABT-578 epimers. Under chromatographic conditions, each isomer/epimer can also show pyrane and oxepane form. The number of potential observed process isomers/epimers can be calculated using the following rule: ABT-578 can have $2 \times (2^n - 1)$ of epimer impurities (where n is number of active chiral centers) [22]. N2 isomer can have 2×2^n N2 epimer impurities. With $n = 4$, 62 (30 from ABT-578 and 32 form N2-isomer) impurities with the same MS of ABT-578 can be potentially observed. Previous literature has reported studies of complex MS/MS fragmentation patterns of a few metabolic compounds of rapamycin and everolimus, and indicated that overlap of chromatographic metabolic impurity peaks made the interpretation of MS spectra nearly impossible. Therefore, it is critical that a HPLC system provide the highest resolution and sensitivity for metabolic compounds analyses [23–25]. Other literature also has reported studies of HPLC-UV and HPLC-MS for therapeutic drug monitoring of everolimus [26,27]. As indicated, a strategy for process impurity tracking is generally via molecular ion identification [14,28]. In this complex ABT-578 process, tracking and mapping impurities of numerous isomers/epimers (co-elution) with mainly a MS/MS approach is simply not realistic or useful. In the article, single MS data information with positive and negative mode is used, in conjunction with DAD. Fig. 13 shows unique MS spectra of ABT-578 pyran form and oxepane form in both positive and negative mode under Method A conditions. Similar MS spectra are also observed under Method B conditions. MS/MS of ABT-578 pyran and oxepane, and N2 isomer, and some epimers revealed the same MS spectra (data not show). Table 2 illustrates an example of the type of collective mapping information that can be gained, from early process to final API, made possible by HPLC-UV-MS detection (positive mode and negative mode applied throughout the process) for most important known and unknown impurities.

4. Conclusion

ABT-578 is a semi-synthetic tetrazole analog of the fermentation product rapamycin, with 15 chiral centers and several reactive sites. It is manufactured in a relatively short process that has many complexities due to the nature of the polyene macrolide core and its susceptibility to change. There are multiple opportunities for related impurities to arise from starting material of rapamycin and during the formation of ABT-578 subsequent processing. ABT-578 and its related impurities are not easily separated. Their structural differences are typically minor and tend not to provide substantial differentiation in terms of UV spectrum or chromatographic behavior. In order to map and

understand the process, complimentary HPLC-UV-MS methods were employed to track impurities. Method A, RP-HPLC-UV-MS, 210 nm, as a stability indicating method, separates most general impurities. Method B, NP-HPLC-UV-MS, 278 nm, as a screening method and a targeted method, separates isomers of repacking and epimers of ABT-578, as well as reactive intermediates. And Method C, RP-HPLC-UV, 265 nm, as a targeted method, separates highly polar impurities. With the capability of MS detection, the process of distinguishing and tracking known and unknown impurities was greatly facilitated, as well as mapping all key process impurities (Fig. 2b and Table 2). This combination of technology helped bring about extensive process understanding with correlation to API impurity profile, and also validates the emerging strategy of generally applying HPLC-UV-MS methodology to API processes and in-process materials.

Acknowledgements

The authors wish to thank Steven Nowak, David Werst, and Quan Chen from Abbott Vascular Division; Sanjay Chemburkar and David Li from Abbott Global Pharmaceutical Operations, for their contributions and helpful discussions in early stages of method development. The authors also wish to thank Paul West from Abbott Structural Chemistry Department, Global Pharmaceutical Research and Development, for helpful MS discussion.

References

[1] M.J. Eisenberg, K.J. Konnyu, Am. J. Cardiol. 98 (3) (2006) 375.
[2] S.E. Burke, R.E. Kuntz, L.Z. Schwartz, Adv. Drug Deliv. Rev. 58 (3) (2006) 437.
[3] R.W. Rickards, R.M. Smith, B.T. Golding, J. Antibiot. 12 (1970) 603.
[4] B.A. Olsen, Pharm. Technol., Scaling up Manufacture Process, 2005, p. 14.
[5] S. Ahuja, K.M. Alsante, Handbook of Isolation and Characterization of Impurities in Pharmaceutical, Academic Press, San Diego, California, 2003, p. 89.
[6] M.J. Hilhorst, G.W. Somsen, G.J. de Jong, Electrophoresis 22 (2001) 2542.
[7] J. Ermer, M. Vogel, Biomed. Chromatogr. 16 (2000) 373.
[8] S. Gorog, Curr. Trend Anal. Chem. 1 (1998) 11.
[9] C. Ecker, N. Haskins, J. Langridge, Rapid Commun. Mass Spectrom. 11 (1997) 1916.
[10] C. Ecker, K.A. Hutton, V. de Biasi, P.B. East, N.J. Haskins, V.W. Jacewicz, J. Chromatogr. A 686 (1994) 213.
[11] E.C. Nicolas, T.H. Scholz, J. Pharm. Biomed. Anal. 16 (1998) 825.
[12] J.K. Strasters, H.A.H. Billet, L. De Galan, B.G.M. Vandeginste, J. Chromatogr. 499 (1990) 499.
[13] IUPAC Nomenclature of Organic Chemistry, A Guide to IUPAC Nomenclature of Organic Components (Recommendations 1993), Blackwell Scientific Publications, Boston, MA, 1993.
[14] G. Xue, A.D. Bendick, R. Chen, S.S. Sekulic, J. Chromatogr. A 1050 (2004) 159.
[15] R. Nageswara Rao, V. Nagaraju, J. Pharma. Biomed. Anal. 33 (2003) 335.
[16] G. Robert, L. Fan, V.P. Shevchenko, I. Yu, Nagaev, N.F. Myasoedov, A.B. Susan, J. Label. Compd. Radiopharm. 49 (2006) 849.
[17] R. Wagner, K.W. Mollison, L.L. Liu, C.L. Henry, T.A. Rosenberg, N. Bamaung, N. Tu, P.E. Wiedeman, Y. Or, J.E. Luly, B.C. Lane, J. Trevillyan, Y.W. Chen, T. Fey, G. Hsieh, K. Marsh, M. Nuss, P.B. Jacobson, D. Wilcox, R.P. Carlson, G.W. Carter, S.W. Djuric, Bioorg. Med. Chem. Lett. 15 (2005) 5340.
[18] K.W. Mollison, A.M. LeCaptain, S.E. Burke, K.R. Cromack, P.J. Tarcha, Medical Devices Containing Rapamycin Analog, United State Patent Application Publication, US 2005/0175600/A1.
[19] K.W. Mollison, Tetrazole-Containing Rapamycin Analog with Shorted Half-Lives, United State Patent, US 6015815 (2000).
[20] M.K. Dhaon, C.C. Zhou, S. Chemburkar, H. Morton, Tetrahedron Lett. 48 (2007) 1059.
[21] L.R. Snyder, J.J. Kirkland, J.L. Glajch, Practical HPLC Method Development, John Wiley & Sons, Inc., New York, NY, 1997, p. 733.
[22] R.C. Williams, C.M. Riley, K.W. Sigvardson, J. Fortunak, P. Ma, E.C. Nicolas, S.E. Unger, D.F. Krahn, S.L. Bremner, J. Pharma. Biomed. Anal. 17 (1998) 917.
[23] K.O. Boernsen, W. Egge-Jacobsen, B. Inverardi, T. Strom, F. Streit, H.M. Schiebel, L.Z. Benet, U. Chriatians, J. Mass. Chem. 42 (2007) 793.
[24] K. Hallensleben, M. Raida, G. Habermehl, J. Am. Soc. Mass Spectrom. 11 (2000) 516.
[25] F. Streit, U. Christians, H.M. Schiebel, A. Meyer, K.F. Sewing, Drug Metab. Dispos. 24 (1996) 1272.
[26] P.J. Taylor, M.E. Franklin, K.S. Graham, P.I. Pillans, J. Chromatogr. B 848 (2007) 208.
[27] S. Baldelli, S.M. Urgia, S. Merlini, S. Zenoni, N. Perico, G. Remuzzi, D. Cattaneo, J. Chromatogr. B 816 (2005) 99.
[28] M. Argentine, P.K. Owens, B.A. Olsen, Adv. Drug Deliv. Rev. 59 (2007) 12.